

## Significance of Na<sup>+</sup> current in the excitability of atrial and ventricular myocardium of the fish heart

Jaakko Haverinen and Matti Vornanen\*

University of Joensuu, Department of Biology, PO Box 111, 80101 Joensuu, Finland

\*Author for correspondence (e-mail: matti.vornanen@joensuu.fi)

Accepted 13 December 2005

### Summary

The present study examines the importance of the Na<sup>+</sup> current ( $I_{Na}$ ) in the excitability of atrial and ventricular myocardium of the rainbow trout heart. Whole-cell patch-clamp under reduced sarcolemmal Na<sup>+</sup> gradient showed that the density of  $I_{Na}$  is similar in atrial and ventricular myocytes of the trout heart, and the same result was obtained when  $I_{Na}$  was elicited by chamber-specific action potentials (AP) in normal physiological saline solution. However, the maximum rate ( $V_{max}$ ) of AP upstroke, measured with microelectrodes in intact trout heart, was 21% larger in atrium than ventricle, and thus in variance with the similar  $I_{Na}$  density of the two myocyte types. Furthermore,  $V_{max}$  calculated from the  $I_{Na}$  was 2.1 and 3.2 times larger for atrium and ventricle, respectively, than the values obtained from the APs. The discrepancy between  $I_{Na}$  of isolated myocytes and  $V_{max}$  of intact muscle

is only partly explained by the inward rectifier K<sup>+</sup> current ( $I_{K1}$ ), which overlaps  $I_{Na}$  and decreases the net depolarising current. Clear differences exist in the voltage dependence of steady-state activation and inactivation as well as in the inactivation kinetics of  $I_{Na}$  between atrial and ventricular myocytes. As a result of a more negative voltage dependence of  $I_{Na}$  activation, smaller  $I_{K1}$  and higher input resistance of atrial myocytes, the voltage threshold for AP generation is more negative in atrium than ventricle of the trout heart. These findings suggest that atrial muscle is more readily excitable than ventricular muscle, and this difference is partly due to the properties of the atrial  $I_{Na}$ .

Key words: trout heart, sodium current, action potential upstroke, impulse conduction, *Oncorhynchus mykiss*.

### Introduction

The generation of action potentials (AP) and synchronized spread of excitation are essential features for the coordinated pumping action of the heart. The spontaneous rhythm of the heart is generated by pacemaker cells that produce slow APs which excite atrial myocytes to produce fast but short-duration APs (Irisawa, 1978; Bouman and Jongsma, 1986; Golod et al., 1998). The atrial muscle excitation wave enters the ventricular myocardium, where it produces even quicker rising and more prolonged APs. This sequence of events requires a particular composition of membrane currents from each myocyte type to enable adequate excitability for each cardiac compartment and tuning of excitability and impulse conduction to the unique contractile properties of atrial and ventricular myocardium (Hume and Uehara, 1985; Schram et al., 2002; Marionneau et al., 2005).

The first current to be activated in atrial and ventricular myocytes is the fast Na<sup>+</sup> current ( $I_{Na}$ ), which provides the necessary charge to depolarize the cell membrane and activate other ion channels in the production of chamber-specific APs (Schram et al., 2002; Kleber and Rudy, 2004). Although the properties of  $I_{Na}$  are thought to primarily determine the

excitability of myocytes and conduction velocity of the cardiac AP, the ability of  $I_{Na}$  to depolarize the membrane is also dependent on the K<sup>+</sup> currents and other repolarising currents that are activated in the voltage range of AP onset (Golod et al., 1998). In this regard, the time-independent inward rectifier K<sup>+</sup> current ( $I_{K1}$ ) is particularly important since it generates outward K<sup>+</sup> flux immediately when membrane potential exceeds the reversal potential of K<sup>+</sup> ions. Previous studies have shown that there are dramatic differences in the density of the  $I_{K1}$  between atrial and ventricular myocytes of the trout heart (Vornanen et al., 2002) that might set differential demands on  $I_{Na}$  in regulating excitability of the two cardiac chambers. This prompted us to compare the properties of  $I_{Na}$  in atrial and ventricular myocytes of the rainbow trout heart to identify the relative role of chamber-specific  $I_{Na}$  in the depolarisation of the fish heart. In addition to Na<sup>+</sup> and K<sup>+</sup> currents, factors that may not necessarily be inherent to isolated myocytes, such as intercellular electric coupling between myocytes and non-myocyte cells, are likely to affect AP generation (Camelliti et al., 2005). Therefore, the rate of AP upstroke of intact atrium and ventricle were compared to the theoretical values obtained from the density of  $I_{Na}$  in isolated myocytes.

## Materials and methods

### Fish

Rainbow trout (*Oncorhynchus mykiss* Walbaum) were obtained from a local fish farm near the University of Joensuu (Finland). In the lab, fish (257.16±12.13 g,  $N=27$ ) were reared in temperature-controlled 1000 litre stainless steel tanks with a continuous supply of aerated groundwater at the rate of 0.5 l min<sup>-1</sup>. Fish were held for at least 4 weeks at constant temperature (4°C) under a 15 h:9 h light:dark photoperiod before experimentation. During that time, trout were fed five times per week *ad libitum* with commercial fish fodder (Biomar, Brande, Denmark).

### Myocyte isolation

Atrial and ventricular myocytes were enzymatically isolated using previously published methods (Vornanen, 1997). Briefly, fish were stunned with a blow to the head, the spine was cut and the heart was excised. A metallic cannula was advanced through the bulbus arteriosus into the ventricle, and the heart was retrogradely perfused first with a nominally Ca<sup>2+</sup>-free, low-Na<sup>+</sup> solution (containing in mmol l<sup>-1</sup>: 100 NaCl, 10 KCl, 1.2 KH<sub>2</sub>PO<sub>4</sub>, 4 MgSO<sub>4</sub>, 50 taurine, 20 glucose and 10 Hepes at pH 6.9 at 20°C) for 10 min and then with a fresh low-Na<sup>+</sup> solution supplemented with 0.75 mg ml<sup>-1</sup> collagenase (Type IA, Sigma, St Louis, MO, USA), 0.5 mg ml<sup>-1</sup> trypsin (Type IX, Sigma) and 0.5 mg ml<sup>-1</sup> fatty-acid-free bovine serum albumin for 15 min from a height of 50 cm. Both solutions were oxygenated with 100% O<sub>2</sub>, and the enzyme solution was recycled using a peristaltic pump. After enzymatic digestion, atrium and ventricle were excised, placed in fresh low-Na<sup>+</sup> solution in a Petri dish and cut into small pieces with scissors. Single cells were released by agitating tissue pieces through the opening of a Pasteur pipette. Myocytes were stored at 6°C and used within 8 h of isolation. All experiments were performed with the consent of the local committee for animal experimentation.

### Whole-cell patch-clamp experiments

A small sample of myocyte suspension was transferred to a recording chamber (RC-26; Warner Instrument Corp., Hamden, CT, USA; volume 150 µl) and cells were allowed to settle on the chamber bottom before superfusing with external saline solutions at a rate of 1.5–2.0 ml min<sup>-1</sup>. First, the myocytes were perfused with normal K<sup>+</sup>-based saline (containing in mmol l<sup>-1</sup>: 150 NaCl, 5.4 KCl, 1.8 CaCl<sub>2</sub>, 1.2 MgCl<sub>2</sub>, 10 glucose, 10 Hepes, 0.01 nifedipine, pH adjusted to 7.7 with NaOH), where gigaohm seal and whole-cell patch-clamp recording of the myocytes were established. Internal perfusion of the myocytes with pipette solution (containing in mmol l<sup>-1</sup>: 5 NaCl, 130 CsCl, 1 MgCl<sub>2</sub>, 5 EGTA, 5 Mg<sub>2</sub>ATP, 5 Hepes, pH adjusted to 7.2 with CsOH) continued for at least 3 min in order to allow buffering of intracellular Ca<sup>2+</sup> with 5 mmol l<sup>-1</sup> EGTA. Then, solution flow could be switched to a low-Na<sup>+</sup> external solution (containing in mmol l<sup>-1</sup>: 20 NaCl, 120 CsCl, 1 MgCl<sub>2</sub>, 0.5 CaCl<sub>2</sub>, 10 glucose, 10 Hepes, 0.01 nifedipine, pH adjusted to 7.7 with CsOH) without inducing

contracture in the patched myocyte.  $I_{Na}$  was recorded in the low-Na<sup>+</sup> saline solution at 4°C (Haverinen and Vornanen, 2004).

The whole-cell voltage-clamp measurements of  $I_{Na}$  were performed using an Axopatch 1-D amplifier with a CV-4 1/100 headstage (Axon Instruments, Union City, CA, USA). The digitised data were stored on the hard drive of the computer using the Clampex 8.2 software (Axon Instruments). The recordings were analysed off-line with Clampfit 8.2 and SigmaPlot 6.0 (SPSS, Inc., Chicago, IL, USA) software. Patch pipettes were pulled from borosilicate glass (Garner, Claremont, CA, USA) using a vertical two-stage puller (L/M-3P-A; List-Electronic, Darmstadt, Germany). Offset potentials were zeroed just before the formation of gigaohm seal, and the pipette capacitance (7.43±0.08 pF,  $N=108$ ) was compensated for after the seal formation. The membrane was ruptured by a short voltage pulse (zap), and capacitive transients were eliminated by adjusting series resistance and cell capacitance compensation circuits. Mean resistance of the electrodes and total access resistance before compensation were 3.23±0.06 and 9.88±0.12 MΩ ( $N=108$ ), respectively.  $I_{Na}$  was elicited from the holding potential of -120 mV with different pulse protocols and recorded at a sampling rate of 10 kHz. The recordings were low-pass filtered at 5 kHz. The calculated liquid-junction potential of the electrodes was about 1.5 mV, which was not corrected in the results.

Low external Na<sup>+</sup> concentration (20 mmol l<sup>-1</sup>), low experimental temperature (4°C) and relatively small size of the myocytes (51.08±1.45 and 53.50±1.95 pF for atrial and ventricular myocytes, respectively) kept the size of  $I_{Na}$  small (<2 nA) and allowed adequate voltage control of the current (maximally a 2-mV error with 10 MΩ access resistance). To ensure good voltage control, a minimum of 80% series resistance compensation was routinely applied.

### Steady-state activation and inactivation of $I_{Na}$

Steady-state inactivation was determined using a two-step protocol where a 500 ms conditioning pulse to potentials between -110 mV and -20 mV was followed by a 15 ms test pulse to -20 mV. For the voltage dependence of steady-state inactivation, the normalized test pulse currents ( $I/I_{max}$ ) were plotted as a function of membrane potential and fit to the Boltzmann equation:

$$y = 1 / [1 + \exp(V - V_{0.5}) / -S], \quad (1)$$

where  $V$  is membrane potential,  $V_{0.5}$  is the midpoint and  $-S$  is the slope of the curve. The steady-state voltage dependence of activation was obtained by plotting the normalized conductance ( $G/G_{max}$ ) as a function of membrane potential and fitting it to the Boltzmann distribution (above) with a positive slope ( $S$ ). The voltage dependence of Na<sup>+</sup> channel conductance was obtained from the current–voltage relationships according to the equation:

$$G_{Na} = I_{Na} / (V - V_{rev}), \quad (2)$$

where  $G_{Na}$  is the Na<sup>+</sup> conductance of the membrane,  $I_{Na}$  is the

peak  $\text{Na}^+$  current at a given membrane potential ( $V$ ) and  $V_{\text{rev}}$  is the reversal potential of  $I_{\text{Na}}$ .

#### Inactivation of $I_{\text{Na}}$

The development of rested-state inactivation was examined by a protocol that consisted of a conditioning prepulse from  $-120$  to  $-80$  mV with variable (30–360 ms) duration, followed by a short return (3 ms) to the holding potential and a test pulse to  $-20$  mV for 30 ms. The peak  $I_{\text{Na}}$  elicited by test pulses was plotted as a function of the prepulse duration and fit to a single exponential function to obtain the time constant for the development of rested-state inactivation. Time-dependent recovery of  $I_{\text{Na}}$  from inactivation was examined using a paired-pulse protocol where two successive 100 ms pulses from  $-120$  to  $-20$  mV were separated by a variable (40–400 ms) delay at  $-82$  mV. The peak  $I_{\text{Na}}$  during the latter pulse was plotted as a function of time and fit to a single exponential function ( $y=y_0+a^{-bt}$ ) to obtain the time constant ( $\tau=1/-b$ ) of recovery from inactivation.

The time constants of  $I_{\text{Na}}$  inactivation kinetics were derived by fitting the decay phase of the  $I_{\text{Na}}$  at different membrane potentials ( $-40$  to  $+10$  mV) with a single exponential equation using the Chebyshev transformation procedure of the Clampfit software package. The kinetics of  $I_{\text{Na}}$  activation was assessed by determining the time from the start of voltage-clamp pulse to the peak inward current at  $-40$  to  $+10$  mV.

#### Voltage threshold of the net inward current

The depolarising power of  $I_{\text{Na}}$ , in the presence of all ion currents of the cardiac myocyte, was determined by measuring the threshold voltage for net inward current in normal physiological saline (see recording of APs) in the absence of channel blockers. Pipette solution in these experiments contained (in  $\text{mmol l}^{-1}$ ): 140 KCl, 5  $\text{Na}_2\text{ATP}$ , 1  $\text{MgCl}_2$ , 0.03 Tris-GTP, 10 HEPES and pH adjusted to 7.2 with KOH. Currents were elicited from the resting membrane potential of  $-82$  mV with 30 ms depolarising pulses at 2 mV increments. Membrane time constant ( $\tau$ ) and series resistance of atrial and ventricular myocytes were determined from small sub-threshold depolarisations. Input resistance ( $M\Omega$ ) of atrial and ventricular cells was calculated by using the equation  $R=\tau/\text{cell size}$ , where  $\tau$  is in s and cell size is in pF.

#### Recording of action potentials

Atrial and ventricular APs were recorded from multicellular preparations. The whole heart was excised, and the ventricle was cut into two parts to allow free access of oxygenated (100%  $\text{O}_2$ ) solution to the tissue. The heart was fixed with insect pins on the Sylgaard<sup>TM</sup>-coated bottom of the 15-ml recording chamber filled with physiological saline (in  $\text{mmol l}^{-1}$ ): 150 NaCl, 3 KCl, 1.2  $\text{MgSO}_4$ , 1.2  $\text{NaH}_2\text{PO}_4$ , 1.8  $\text{CaCl}_2$ , 10 HEPES and 10 glucose adjusted to pH 7.7 with NaOH. The spontaneously beating heart was allowed to equilibrate at  $4^\circ\text{C}$  for about 1 h to reach a stable heart rate ( $31.2\pm 1.2$  beats  $\text{min}^{-1}$ ). APs were recorded with sharp microelectrodes filled with 3  $\text{mol l}^{-1}$  KCl. Analogue signals

were amplified by a high-impedance amplifier (KS-700; WPI, Sarasota, FL, USA) and digitized (Digidata-1200 AD/DA board; Axon Instruments) with a sampling rate of 2 kHz before storing on the computer with the aid of Axotape (Axon Instruments Inc., Union City, CA, USA) acquisition software. The maximum rate of AP upstroke ( $V_{\text{max}}$ ) was obtained by differentiation of the voltage signal in SigmaPlot. The  $V_{\text{max}}$  measured in intact tissue was compared to the theoretical value  $V_{\text{max}}$  obtained from the peak  $I_{\text{Na}}$  under AP clamp according to the relationship between membrane voltage ( $V_m$ ), membrane

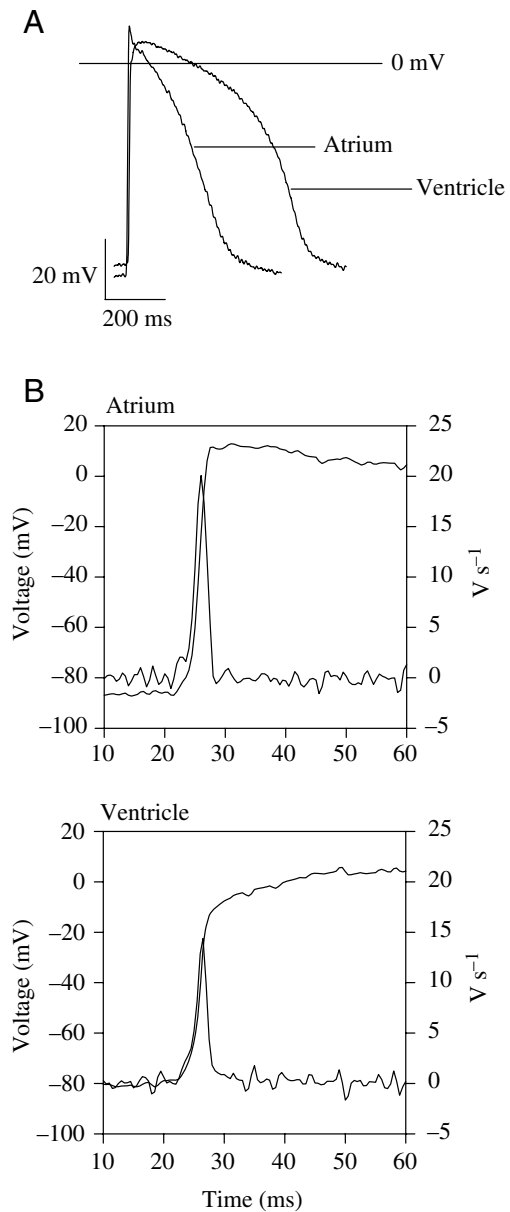


Fig. 1. Action potentials of the rainbow trout heart. Action potentials were recorded with microelectrodes from intact cardiac tissue at  $4^\circ\text{C}$ . (A) Representative recordings of atrial and ventricular action potentials. (B) The rising phase of atrial and ventricular action potentials and their first derivatives, indicating the rate of action potential upstroke.

Table 1. Action potential characteristics of atrial and ventricular muscle and the threshold voltage for the net inward current in atrial and ventricular myocytes of the rainbow trout heart

	Atrium	N	Ventricle	N
Resting potential (mV)	-83.29±0.45*	12	-81.54±0.39	12
Action potential				
Amplitude (mV)	94.63±1.92*	12	88.67±1.01	12
Overshoot (mV)	11.58±1.27	12	8.41±1.02	12
APD at 0 mV (ms)	136.37±21.28*	12	363.13±31.23	12
APD50 (ms)	306.39±4.81*	12	705.16±11.48	12
V <sub>max</sub> (V s <sup>-1</sup> )	20.19±1.18*	12	16.05±0.88	12
Cell size (pF)	51.08±1.45	24	53.50±1.95	19
Threshold voltage (mV) for the net inward current (HP=-82 mV)	-48.75±1.80	12	-45.73±1.39	13
Time constant (τ)	58.79±4.70*	10	7.14±0.68	16
Input resistance (MΩ)	1150.95±91.93*	10	133.46±12.62	16

All experiments were conducted at 4°C. A statistically significant difference ( $P<0.05$ ) between atrial and ventricular myocytes is indicated by an asterisk.

capacitance ( $C_m$ ) and membrane current:  $dV_m/dt = -I_{Na}/C_m$ . The value of specific membrane capacitance was taken to be 1.59 pF mm<sup>-2</sup> (Vornanen, 1997).

#### Statistical analyses

Mean values between atrial and ventricular myocytes and between controls and treatments were compared with Student's *t*-test for unpaired data. *P* values of <0.05 were regarded as statistically significant. Data are presented as means ± s.e.m.

## Results

### Characteristics of atrial and ventricular action potentials

Action potentials recorded with sharp microelectrodes from intact atrium and ventricle (at 4°C) are strikingly different. Ventricular AP is approximately double in duration and has a

smaller amplitude and slightly less negative resting membrane potential (RMP) in comparison with atrial AP (Fig. 1A; Table 1). In both cardiac compartments, the  $V_{max}$  occurred at the membrane potential of -20 mV, but the absolute rate was 21% faster in atrium than ventricle ( $P<0.05$ ) (Fig. 1B), suggesting differences in net depolarising current.

### Size and voltage-dependence of $I_{Na}$

The current-voltage relationships of  $I_{Na}$  in atrial and ventricular myocytes are shown in Fig. 2A.  $I_{Na}$  activated near -70 mV, peaked at about -20 mV and reversed close to the theoretical reversal potential (32 mV) of  $I_{Na}$ . At negative voltages, atrial  $I_{Na}$  was significantly larger than ventricular  $I_{Na}$ . Furthermore, the half-voltages ( $V_{0.5}$ ) of both steady-state activation and inactivation were about 6 mV more negative in atrial than ventricle myocytes (Fig. 2B; Table 2). However, the peak density of  $I_{Na}$  was similar in both myocyte types and thus

Table 2. Comparison of the  $I_{Na}$  in atrial and ventricular myocytes of the rainbow trout heart

	Atrial myocytes	N	Ventricular myocytes	N
$G_{max}$ (pS pF <sup>-1</sup> )	0.42±0.03	14	0.39±0.02	13
Steady-state activation				
$V_{0.5}$ (mV)	-39.48±1.00*	14	-33.94±2.56	12
Slope	7.02±0.53	14	6.20±0.23	12
Steady-state inactivation				
$V_{0.5}$ (mV)	-84.88±1.01*	13	-79.61±1.37	12
Slope	5.66±0.43	13	5.79±0.29	12
Rested-state inactivation, τ (ms)	65.90±8.24*	13	73.50±5.03	12
Recovery from inactivation, τ (ms)	46.53±7.24	9	60.72±13.12	9

A statistically significant difference ( $P<0.05$ ) between atrial and ventricular myocytes is indicated by an asterisk.  $G_{max}$ , the maximal conductance of  $I_{Na}$ .

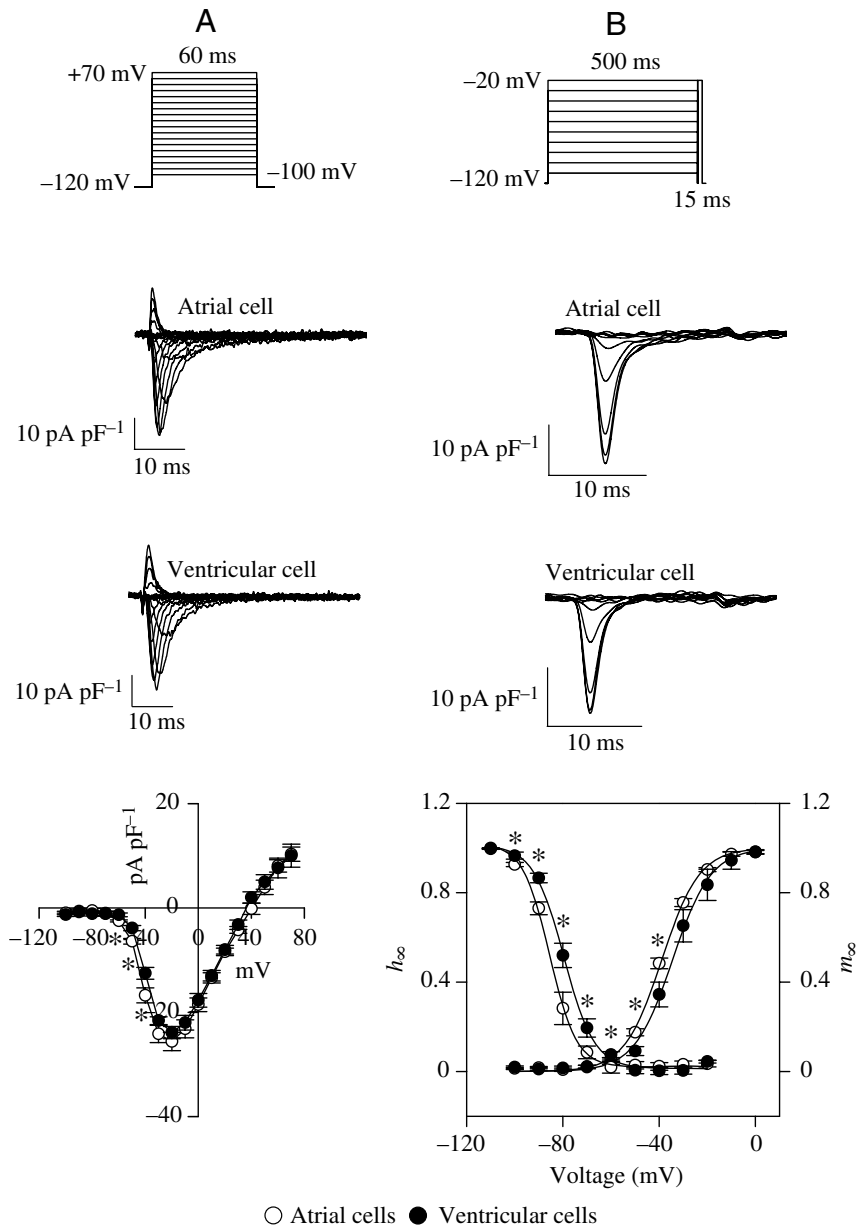


Fig. 2. Comparison of voltage-dependent properties of  $I_{Na}$  between atrial and ventricular myocytes of the rainbow trout heart. Current-voltage relationships and steady-state activation  $m_{\infty}$  and inactivation curves  $h_{\infty}$  of the  $I_{Na}$  are shown in A and B, respectively. Voltage protocols (top), representative recordings (middle) and mean results ( $\pm$  s.e.m.;  $N=12-14$ ) (bottom) are shown. Asterisks show a significant difference ( $P<0.05$ ) between atrial and ventricular myocytes.

than ventricular myocytes in accordance with the availability curves (Fig. 3A). In contrast to the development of the rested-state inactivation, the time constant of recovery from  $I_{Na}$  inactivation at  $-82$  mV was similar in ventricular and atrial myocytes (Fig. 3B; Table 2).

Inactivation kinetics was examined in a voltage range from  $-40$  to  $+10$  mV. At 0 and  $+10$  mV, where all  $Na^+$  channels are activated, the kinetics of inactivation was faster in ventricular than atrial myocytes (Fig. 4). That the differences were not seen at other voltages is likely due to the 6 mV difference in the voltage position of steady-state activation curve, which might obscure the faster inactivation of ventricular  $I_{Na}$  at more negative voltages. No differences were found in activation kinetics.

#### $I_{Na}$ under action potential clamp

As there were differences in RMP, shape of AP, inactivation kinetics and voltage dependence of  $I_{Na}$  between atrium and ventricle,  $I_{Na}$  was next studied under more physiologically relevant conditions.  $I_{Na}$  was elicited at physiological external  $Na^+$  concentration with chamber-specific APs, which were delivered at the physiological

cannot explain the chamber-specific differences in the rate of AP upstroke.

#### Inactivation of $I_{Na}$

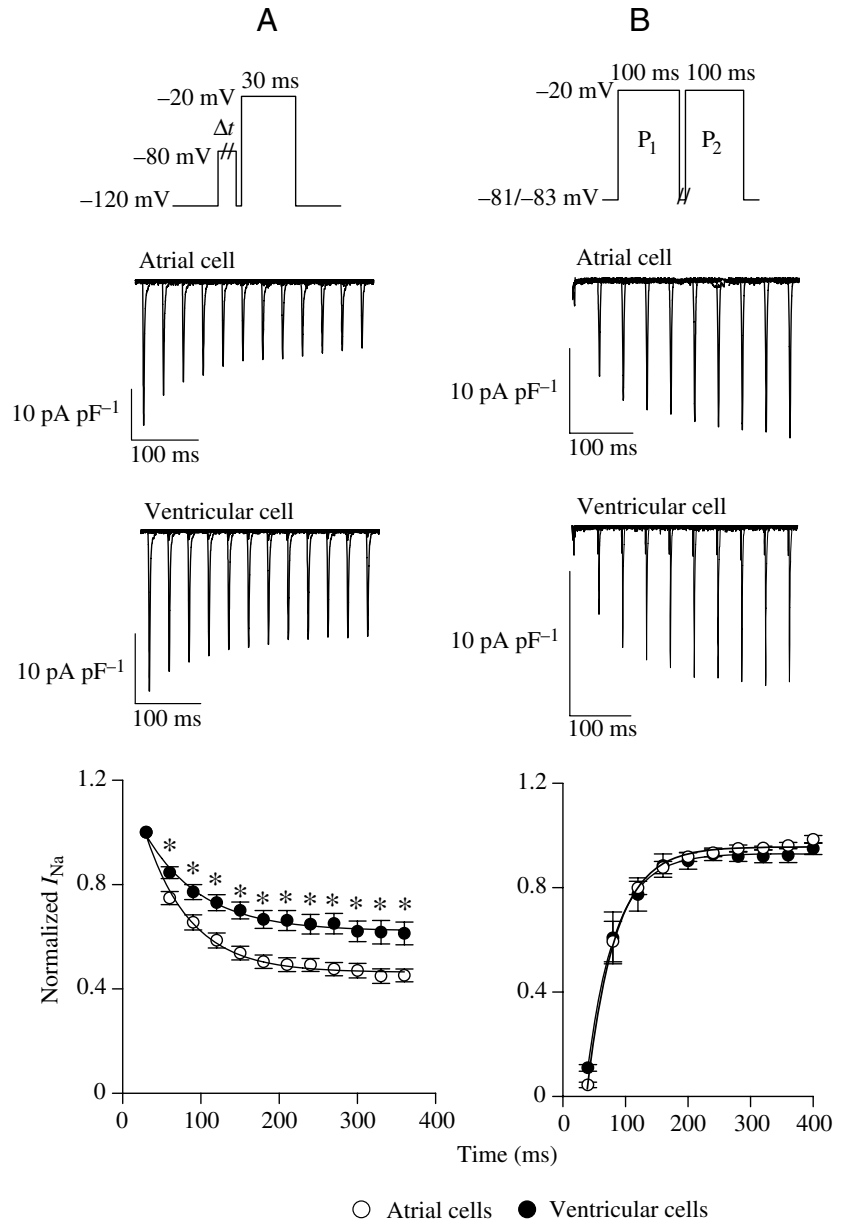
In order to clarify whether differences in the time domain of  $I_{Na}$  could be responsible for differences in  $V_{max}$ , we examined the inactivation of  $I_{Na}$ . The rate of transfer of  $Na^+$  channels from resting closed state to the inactivated closed state was measured by clamping the membrane potential from  $-120$  to  $-80$  mV for different durations and then recording the  $I_{Na}$  at  $-20$  mV. Since the opening of  $Na^+$  channels is unlikely at  $-80$  mV (Fig. 1A), the decrease in amplitude of  $I_{Na}$  as a function of prepulse duration is most likely due to the direct transfer of  $Na^+$  channels from resting closed state to inactivated closed state without intervening opening. At  $-80$  mV, the development of rested-state inactivation of  $I_{Na}$  was faster and more extensive in atrial

beating frequency of 0.3 Hz. The peak density of  $I_{Na}$  and the maximum rate of membrane depolarization calculated from  $I_{Na}$  were not significantly different between atrial and ventricular myocytes (Fig. 5). These findings indicate that the size of  $I_{Na}$  under physiologically realistic conditions does not differ between atrium and ventricle and cannot therefore be responsible for the differences in  $V_{max}$  found in intact atrium and ventricle. Interestingly, the  $V_{max}$  calculated from the peak  $I_{Na}$  was 2.1 and 3.2 times larger, for atrium and ventricle, respectively, than the  $V_{max}$  measured in the intact tissue, suggesting the presence of repolarising current(s) and/or other effects that antagonize  $I_{Na}$  *in situ* (Fig. 5).

#### Voltage threshold for the net inward current

To be able to elicit an AP, the amplitude of  $I_{Na}$  must exceed the conductance of simultaneously activated outward currents.

Fig. 3. Time-dependent properties of  $I_{Na}$  in atrial and ventricular myocytes of the rainbow trout heart. (A) Development of rested-state inactivation of  $I_{Na}$ . Increased duration of the prepulse at  $-80$  mV reduces  $I_{Na}$  elicited by the test pulse to  $-20$  mV for 30 ms. (B) Recovery of  $I_{Na}$  from inactivation (reactivation). The amplitude of  $I_{Na}$  elicited by test pulses to  $-20$  mV for 100 ms increases as a function of the time interval between the prepulse  $P_1$  and the test pulse  $P_2$ . Voltage protocols of  $I_{Na}$  are shown at the top, representative recordings in the middle and mean ( $\pm$  s.e.m.) results from 9–14 myocytes at the bottom. Asterisks show a significant difference ( $P < 0.05$ ) between atrial and ventricular myocytes.



In order to determine the voltage threshold for the net inward current, small depolarising pulses were delivered with 2 mV increments to the cells from the resting membrane potential ( $-82$  mV) in the presence of normal physiological levels of external  $Na^+$ ,  $K^+$  and  $Ca^{2+}$ . The net outward current between  $-70$  and  $-50$  mV was bigger and the voltage threshold for the net inward current more positive in ventricular *versus* atrial cells (Fig. 6; Table 2), suggesting that differences in repolarising currents might contribute to the differences in AP generation between atrium and ventricle. Furthermore, the input resistance of the atrial myocytes was almost an order of magnitude larger than that of the ventricular myocytes.

### Discussion

Voltage-gated  $Na^+$  channels determine the rate and extent of the AP upstroke, which are important in the control of impulse conduction velocity and in the maintenance of appropriate waves of excitation through different compartments of the working heart (Fozzard, 1977). Atrial and ventricular muscle have specialized functions for cardiac pumping and therefore have different contractile and electrical properties, which are likely to set chamber-specific demands on the  $Na^+$  channels. The aim of this study was to analyze putative atrio-ventricular differences in the function of  $Na^+$  channels and relate them to the functional heterogeneity of atrial and ventricular tissue in the whole heart. Indeed, the present results indicate that the properties of  $I_{Na}$  are different in atrial and ventricular myocytes of the trout heart, similar to what has recently been described for mammals (Li et al., 2002). Thus, in general,  $I_{Na}$  heterogeneity may be necessary to satisfy the demands of electrical excitability in the functionally specialized compartments of the vertebrate heart.

#### $I_{Na}$ and the rate of AP upstroke

$I_{Na}$  is the largest inward current in cardiac myocytes and therefore a prime determinant for the rate of AP upstroke and

impulse propagation.  $V_{max}$  in the trout heart ( $16$ – $20$   $V s^{-1}$  at  $4^\circ C$ ) was similar to values previously measured in frog ventricular myocytes ( $26.4$   $V s^{-1}$  at  $15^\circ C$ ; Seyama and Yamaoka, 1988) and in skate (*Dasuyatis akajei*) heart ( $9.5$   $V s^{-1}$  at  $20^\circ C$ ; Seyama and Irisawa, 1967) at low temperatures but more than an order of magnitude smaller than in mammalian heart ( $270$   $V s^{-1}$ ) at  $35^\circ C$  (Kiyosue et al., 1993). The large difference in  $V_{max}$  between mammalian and ectothermic hearts is mostly explained by temperature differences.

The  $V_{max}$  was  $\sim 20\%$  faster in atrial tissue than ventricular tissue from the trout heart. This difference is not, however, readily explained by the properties of  $I_{Na}$ , as the peak density of  $I_{Na}$  was similar in atrial and ventricular myocytes.  $I_{Na}$  is the first depolarising current activated in membrane excitation and elicits all or no AP when its amplitude exceeds the amplitude of

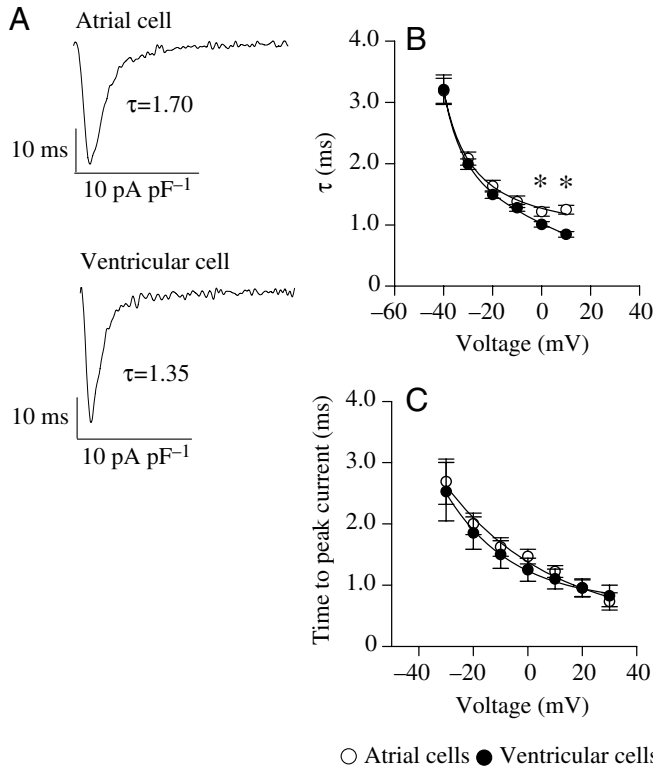


Fig. 4. Voltage dependence of inactivation and activation kinetics of  $I_{Na}$  in atrial and ventricular myocytes of the rainbow trout heart. (A) Representative tracings of  $I_{Na}$  at  $-20$  mV. (B) Mean ( $\pm$  s.e.m.) time constant of inactivation ( $\tau$ ) and (C) time-to-peak current at different voltages. The results are means ( $\pm$  s.e.m.) of 12–14 myocytes. Asterisks show a significant difference ( $P < 0.05$ ) between atrial and ventricular myocytes.

simultaneously activated repolarising currents. Thus, the lower  $V_{max}$  in ventricle might be due to the presence of large repolarising currents that antagonize  $I_{Na}$ . In trout cardiac myocytes, there are two major  $K^+$  currents, the rapid delayed rectifier current,  $I_{Kr}$ , and the background inward rectifier  $K^+$  current,  $I_{K1}$  (Vornanen et al., 2002). The delayed rectifier is a relatively slow, time-dependent current and does not activate to any significant degree during the rapid upstroke of the AP and therefore cannot antagonize  $I_{Na}$ . As a time-independent current,  $I_{K1}$  immediately generates an outward surge of current that overlaps  $I_{Na}$  when the driving force for  $K^+$  efflux is restored by membrane depolarisation (Rasmusson et al., 1990). Previous studies have shown the conductance of  $I_{K1}$  in trout atrial myocytes at  $10^\circ\text{C}$  is less than 5% ( $0.009$  nS  $\text{pF}^{-1}$ ) of its value in ventricular myocytes ( $0.198$  nS  $\text{pF}^{-1}$ ) at the same temperature (Vornanen et al., 2002). Therefore, the greater  $I_{K1}$  of ventricular myocytes might explain in part the difference in  $V_{max}$  between atrial and ventricular muscle of the trout heart. However, the maximum density of the outward  $K^+$  current is small (less than 10%) in comparison to  $I_{Na}$ , and the peak  $I_{K1}$  occurs earlier (around  $-60$  mV) in the AP than the peak  $I_{Na}$  ( $-20$  mV), suggesting that other factors in addition to  $I_{K1}$  might be contributing to the  $V_{max}$  difference between atrium and ventricle.

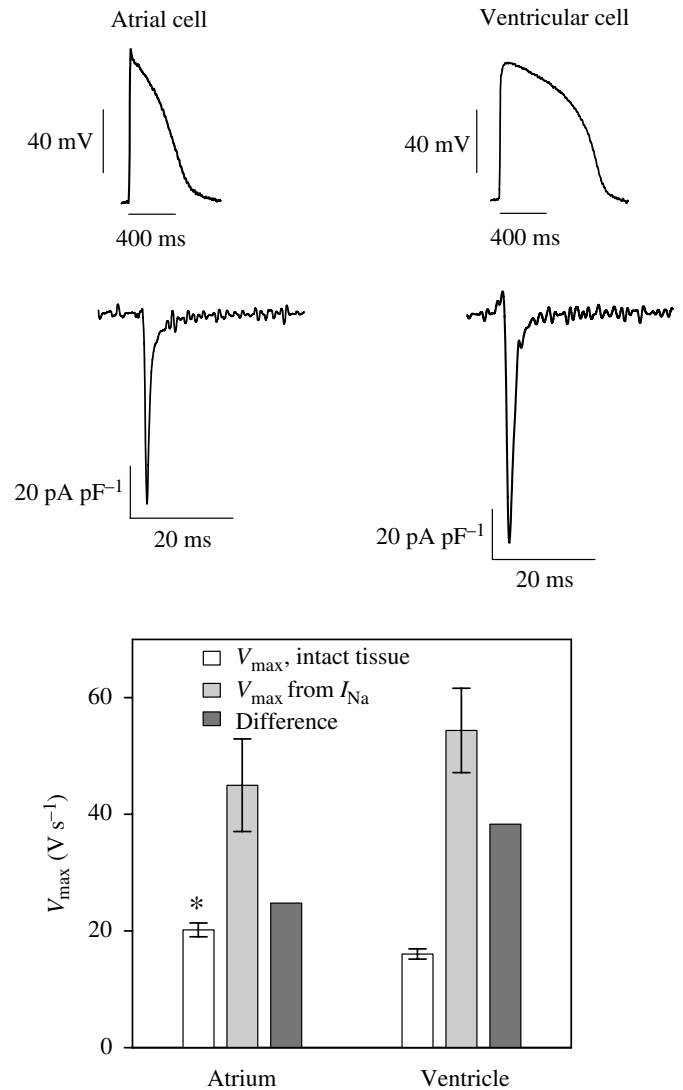


Fig. 5.  $I_{Na}$  under action potential clamp. Representative atrial and ventricular action potentials (top) were used to elicit tetrodotoxin-sensitive  $I_{Na}$  (middle) at physiological external  $\text{Na}^+$  concentration ( $154$  mmol  $\text{l}^{-1}$ ). The bottom panel shows  $V_{max}$  mean ( $\pm$  s.e.m.;  $N=12$ ) calculated from  $I_{Na}$ ,  $V_{max}$  measured in the intact tissue and their difference. Asterisks show a significant difference ( $P < 0.05$ ) between atrial and ventricular myocytes.

Interestingly, the  $V_{max}$  calculated from the density of  $I_{Na}$  in single myocytes was 2–3 times larger than the measured  $V_{max}$  of the intact tissue. The difference between the measured and calculated values could be simply caused by the assumptions made for  $V_{max}$  calculation. If intracellular  $[\text{Na}^+]$  of the intact muscle were substantially higher than the pipette  $[\text{Na}^+]$  ( $10$  mmol  $\text{l}^{-1}$ ), then we could have overestimated physiological  $I_{Na}$  in the patch-clamp experiments. Since intracellular  $[\text{Na}^+]$  of the vertebrate cardiac myocytes is between 4 and 16 mmol  $\text{l}^{-1}$  (usually around 10 mmol  $\text{l}^{-1}$ ; Bers et al., 2003) and doubling of the intracellular  $[\text{Na}^+]$  from 10 to 20 mmol  $\text{l}^{-1}$  would reduce  $\text{Na}^+$  conductance only about 15%, this does not explain the difference. The other possible source of error is the

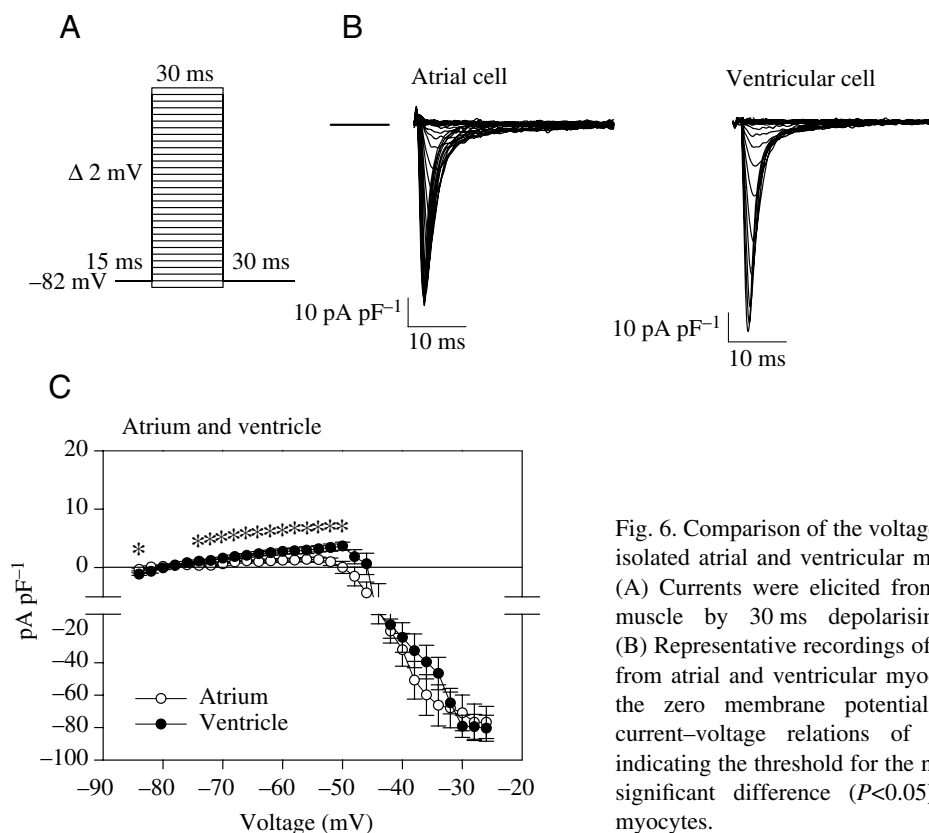


Fig. 6. Comparison of the voltage threshold for net inward current in isolated atrial and ventricular myocytes of the rainbow trout heart. (A) Currents were elicited from the holding potential of  $-82$  mV muscle by 30 ms depolarising pulses in 2 mV increments. (B) Representative recordings of whole-cell membrane currents ( $I_m$ ) from atrial and ventricular myocytes. The horizontal line indicates the zero membrane potential. (C) Mean ( $\pm$  s.e.m.;  $N=6-9$ ) current-voltage relations of atrial and ventricular myocytes indicating the threshold for the net inward current. Asterisks show a significant difference ( $P < 0.05$ ) between atrial and ventricular myocytes.

value of specific membrane capacitance. Instead of the conventional  $1 \text{ pF mm}^{-2}$ , we used the value of  $1.59 \text{ pF mm}^{-2}$  determined for fish cardiac myocytes (Vornanen, 1997). However, the use of the higher capacitance value will decrease, not increase, the difference between measured and calculated  $V_{\max}$ .

In fact, the lower  $V_{\max}$  of intact tissue in comparison to isolated myocytes is an expected finding. Under patch-clamp conditions, the cardiac myocyte is an 'ideally' space-clamped cell, where  $I_{\text{Na}}$  is solely used to change the charge on the membrane capacitance of that particular cell. In multicellular tissue, myocytes are resistively coupled not only to other myocytes but also to cardiac fibroblasts that function as current sinks (Camelliti et al., 2005).  $I_{\text{Na}}$  of the activated myocyte is thus divided between discharging the local membrane capacitance and depolarising the membrane of resistively coupled cells *via* axial current flow (Kleber and Rudy, 2004). Thus, the substantially larger difference between measured and calculated  $V_{\max}$  in ventricle in comparison to atrium suggests that resistive coupling with myocyte and non-myocyte cells might be more extensive in ventricular than atrial myocardium and thus might contribute to lower  $V_{\max}$  of the trout ventricle.

#### *I<sub>Na</sub>* and excitability

Cardiac myocytes are electrically coupled and function both as source and sink for current flow and will therefore affect each other's electrical activity. Apart from its significance in

impulse propagation, the properties of  $I_{\text{Na}}$  affect how different cardiomyocytes interact with each other to guarantee orderly generation and spread of excitation throughout the heart. In this respect, interaction of atrial myocytes with pacemaker cells of the sinus venosus, and interaction of ventricular myocytes with myocytes of the atrioventricular canal, is crucial for function of the fish heart (Arbel et al., 1977; Irisawa, 1978; Sedmera et al., 2003). The excitability of atrial myocyte should be high, so that pacemaker cells are able to securely elicit atrial excitation without any danger of becoming strongly influenced by atrial APs, while excitability of ventricular myocytes might be lower to prevent accidental arrhythmic firing by spontaneous ectopic foci (Joyner et al., 1998). Indeed, the lower voltage threshold for the net inward current of atrial myocytes suggests that they are more readily excited than ventricular myocytes. The low threshold value for AP generation of the atrial myocytes is a function of both a more negative activation threshold of the  $I_{\text{Na}}$  and a smaller  $\text{K}^+$  outward current in the voltage range of the AP threshold in comparison to ventricular myocytes. Furthermore, the very high input resistance of trout atrial myocytes (due to the small  $I_{\text{K1}}$ ) improves atrial excitability.

Taken together, the present results show that voltage dependence of  $I_{\text{Na}}$  is more negative in atrial than ventricular myocytes, but maximum density of  $I_{\text{Na}}$  is similar in both cell types of the trout heart. As a consequence of more negative voltage dependence for  $I_{\text{Na}}$  activation, smaller  $I_{\text{K1}}$  and higher input impedance of atrial myocytes, the current required to

trigger an AP is likely to be smaller in atrial than ventricular myocytes. This makes atrial myocytes readily excitable by pacemaker cells of the sinus venosus. The larger  $V_{\max}$  of atrial muscle cannot be ascribed to the properties of atrial  $I_{\text{Na}}$ , and therefore other factors such as less extensive resistive coupling of atrial myocytes with other myocytes and non-muscle cells and smaller overlapping  $I_{\text{K1}}$  in comparison to ventricular muscle might be involved.

This study was supported by a grant from the Academy of Finland (projects No. 78045 and 210400) to M.V. Anita Kervinen is appreciated for skilful technical assistance.

### References

- Arbel, E. R., Liberthson, R., Langendorf, R., Pick, A., Lev, M. and Fishman, A. P. (1997). Electrophysiological and anatomical observations on the heart of the African lungfish. *Am. J. Physiol.* **232**, H24-H25.
- Bers, D., Barry, W. H. and Despa, S. (2003). Intracellular  $\text{Na}^+$  regulation in cardiac myocytes. *Cardiovasc. Res.* **57**, 897-912.
- Bouman, L. N. and Jongsma, H. J. (1986). Structure and function of the sino-atrial node: a review. *Eur. Heart J.* **7**, 94-104.
- Camelliti, P., Borg, T. K. and Kohl, P. (2005). Structural and functional characterisation of cardiac fibroblasts. *Cardiovasc. Res.* **65**, 40-51.
- Fozzard, H. A. (1977). Heart: excitation-contraction coupling. *Annu. Rev. Physiol.* **39**, 201-220.
- Golod, D. A., Kumar, R. and Joyner, R. W. (1998). Determinants of action potential initiation in isolated rabbit atrial and ventricular myocytes. *Am. J. Physiol.* **274**, H1902-H1913.
- Haverinen, J. and Vornanen, M. (2004). Temperature acclimation modifies  $\text{Na}^+$  current in fish cardiac myocytes. *J. Exp. Biol.* **207**, 2823-2833.
- Hume, J. R. and Uehara, A. (1985). Ionic basis of the different action potential configurations of single guinea-pig atrial and ventricular myocytes. *J. Physiol.* **368**, 525-544.
- Irisawa, H. (1978). Comparative physiology of the cardiac pacemaker mechanism. *Physiol. Rev.* **58**, 461-497.
- Joyner, R. W., Kumar, R., Golod, D. A., Wilders, R., Jongsma, H. J., Verheijck, E. E., Bouman, L., Goolsby, W. N. and van Ginneken, A. C. G. (1998). Electrical interactions between a rabbit atrial cell and a nodal cell model. *Am. J. Physiol.* **274**, H2152-H2162.
- Kiyosue, T., Arita, M., Murumatsu, H., Spindler, A. J. and Noble, D. (1993). Ionic mechanism of action potential prolongation at low temperature in guinea-pig ventricular myocytes. *J. Physiol.* **468**, 85-106.
- Kleber, A. G. and Rudy, Y. (2004). Basic mechanism of cardiac impulse propagation and associated arrhythmias. *Physiol. Rev.* **84**, 431-488.
- Li, G. R., Lau, C. P. and Shrier, A. (2002). Heterogeneity of sodium current in atrial vs. epicardial ventricular myocytes of adult guinea pig hearts. *J. Mol. Cell Cardiol.* **34**, 1185-1194.
- Marionneau, C., Couette, B., Liu, J., Li, H., Mangoni, M. E., Nargeot, J., Lei, M., Escande, D. and Demolombe, S. (2005). Specific pattern of ionic channel gene expression associated with pacemaker activity in the mouse heart. *J. Physiol.* **562**, 223-234.
- Rasmusson, R. L., Clark, J. W., Giles, W. R., Robinson, K., Clark, R. B., Shibata, E. F. and Campbell, D. L. (1990). A mathematical model of electrophysiological activity in a bullfrog atrial cell. *Am. J. Physiol.* **259**, H370-H389.
- Schram, G., Pourrier, M., Melnyk, P. and Nattel, S. (2002). Differential distribution of cardiac ion channel expression as a basis for regional specialization in electrical function. *Circ. Res.* **90**, 939-950.
- Sedmera, D., Reckova, M., De Almeida, A., Sedmerova, M., Biermann, M., Volejnik, J., Sarre, A., Raddatz, E., McCarthy, R. A., Gourdie, R. G. and Thompson, R. P. (2003). Functional and morphological evidence for a ventricular conduction system in zebrafish and *Xenopus* hearts. *Am. J. Physiol.* **284**, H1152-H1160.
- Seyama, I. and Irisawa, H. (1967). The effect of high sodium concentration on the action potential of the skate heart. *J. Gen. Physiol.* **50**, 505-517.
- Seyama, I. and Yamaoka, K. (1988). A study of the electrical characteristics of sodium currents in single ventricular cells of the frog. *J. Physiol.* **401**, 257-275.
- Vornanen, M. (1997). Sarcolemmal Ca influx through L-type Ca channels in ventricular myocytes of a teleost fish. *Am. J. Physiol.* **272**, R1432-R1440.
- Vornanen, M., Ryökynen, A. and Nurmi, A. (2002). Temperature-dependent expression of sarcolemmal  $\text{K}^+$  currents in rainbow trout atrial and ventricular myocytes. *Am. J. Physiol.* **282**, R1191-R1199.